

# Low-Complexity Multiuser QAM Detection for Uplink 1-bit Massive MIMO

Panos N. Alevizos, *Student Member, IEEE*

**Abstract**—This work studies multiuser detection for one-bit massive multiple-input multiple-output (MIMO) systems in order to diminish the power consumption at the base station (BS). A low-complexity near-maximum-likelihood (nML) multiuser detection algorithm is designed, assuming that each BS antenna port is connected with a pair of single-bit resolution analog-to-digital converters (ADCs) and each user equipment (UE) transmits symbols from a quadrature amplitude modulation (QAM) constellation. First, a novel convex program is formulated as a convex surrogate of the ML detector and subsequently solved through an accelerated first-order method. Then, the solution of the convex optimization problem is harnessed to solve a refined combinatorial problem with reduced search space, requiring non-exponential complexity on the number of the UEs. Judicious simulation study corroborates the efficacy of the resulting two-phase detection algorithm. The proposed two-phase algorithm can achieve symbol error rate (SER) performance close to the ML detector, with significantly reduced computation cost compared to the nML detection schemes in prior art.

**Index Terms**—Massive MIMO, maximum-likelihood detection, quadrature amplitude modulation, uplink.

## I. INTRODUCTION

Massive multiple-input multiple-output (MIMO) systems in conjunction with single-bit resolution analog-to-digital converters (ADCs) will be a promising cost-efficient solution for future green cellular networks that support wide bandwidths. In addition to the above, as the in-phase and the quadrature components of the continuous-valued received samples are quantized separately using one-bit ADCs (i.e., zero-threshold comparators) the resulting hardware complexity at the base station (BS) can be sustained to ultra-low levels.

Relevant papers in [1]–[4] offer the current perspective of uplink massive MIMO with one-bit resolution ADCs. Work in [1] designed a low-complexity message-passing one-bit multiuser detector for quadrature phase-shift keying (QPSK) alphabets at the user equipment devices (UEs), demonstrating performance close to the linear minimum mean-squared error (MMSE) detector with reduced computational cost. Subsequent work [2] offered throughput analysis of one-bit multiuser linear detectors in uplink massive MIMO [4], quantifying also the impact of imperfect channel state information (CSI) at the BS. Near-maximum-likelihood (nML) detection is proposed in [3] using a two-stage procedure.

In this paper, we focus on uplink multiuser massive MIMO systems with single-bit ADCs at the BS, assuming that the UEs transmit symbols from a square quadrature amplitude modulation (QAM) constellation. QAM is the dominating modulation scheme in current Long-Term Evolution-Advanced Pro (LTE-A Pro) and future cellular networks [5]. The proposed detector is divided in two phases. In the first phase, a novel convex

optimization formulation is proposed, standing as a convex surrogate of the ML detection rule; the latter is optimal in terms of symbol error rate (SER) but requires exponential computational cost on the number of UEs and a huge number of memory resources at the BS. The relaxed convex program is solved through an accelerated projected gradient method with adaptive restart, achieving close to the optimal convergence rate. In the second phase of the algorithm, the solution of the convex program is harnessed to identify the less-reliable UE symbols and refine their decision estimates via a combinatorial problem with reduced search space. The resulting two-phase detector does not require exponential computational cost on the number of the UEs. Thorough simulation study demonstrates that the proposed detector achieves similar SER performance with the ML detector, and at the same time, significantly reduces the computational cost compared to the nML detection schemes in prior art.

*Notation:* Notation  $\mathbb{R}$ ,  $\mathbb{R}_+$ , and  $\mathbb{C}$ , stands for the set of real, non-negative, and complex numbers, respectively. Nonbold lower-case letters (e.g.,  $x$ ) will stand for variables. Vectors and matrices will be denoted by lower-case (e.g.,  $\mathbf{x}$ ) and capital (e.g.,  $\mathbf{A}$ ), respectively, bold characters. Symbols  $(\cdot)^\top$  and  $(\cdot)^H$  denote the transpose and the conjugate transpose of a vector or matrix, respectively.  $\mathbf{0}_N$  ( $\mathbf{1}_N$ ) and  $\mathbf{I}_N$  denote the  $N$ -dimensional all-zeros (all-ones) vector and the  $N \times N$  identity matrix.  $\mathcal{CN}(\boldsymbol{\mu}, \boldsymbol{\Sigma})$  denotes the proper complex Gaussian distribution while  $\mathcal{N}(\boldsymbol{\mu}, \boldsymbol{\Sigma})$  denotes the (real) Gaussian distribution.  $\bigotimes_{i=1}^N \mathcal{A}_i$  denotes the  $N$ -fold Cartesian product of sets  $\{\mathcal{A}_i\}_{i=1}^N$ .

## II. SYSTEM MODEL AND PROBLEM STATEMENT

We consider an uplink system consisting of a BS, equipped with  $M$  antennas. The BS serves  $K$  UEs, where  $M \gg K$ . For a single channel use, the received signal at the BS,  $\mathbf{y} \in \mathbb{C}^M$ , is given by

$$\mathbf{y} = \mathbf{H} \mathbf{P} \mathbf{x} + \mathbf{n} = \sum_{k=1}^K \sqrt{p_k} \mathbf{h}_k x_k + \mathbf{n}, \quad (1)$$

where  $p_k$  is the transmit power of the  $k$ th UE,  $k \in \{1, 2, \dots, K\}$ ,  $\mathbf{H} = [\mathbf{h}_1 \mathbf{h}_2 \dots \mathbf{h}_K] \in \mathbb{C}^{M \times K}$  is the compound uplink channel matrix consisting of uplink channel vectors  $\mathbf{h}_k \in \mathbb{C}^M$  from the  $k$ th UE to the BS,  $k \in \{1, 2, \dots, K\}$ . Matrix  $\mathbf{P} \in \mathbb{R}_+^{K \times K}$  is a diagonal matrix, whose diagonal elements comprise of  $\{\sqrt{p_k}\}_{k=1}^K$ ;  $\mathbf{n} \sim \mathcal{CN}(\mathbf{0}_M, \sigma^2 \mathbf{I}_M)$  is additive complex Gaussian noise at the BS of variance  $\sigma^2$ , while vector  $\mathbf{x} = [x_1 x_2 \dots x_K]^\top \in \mathbb{C}^K$  comprises of the  $K$  UEs' transmitted symbols. Each  $x_k$  belongs to a normalized square Q-QAM constellation  $\mathcal{X}$ , i.e., vector  $\mathbf{x}$

satisfies  $\mathbb{E}[\mathbf{x}] = \mathbf{0}_K$  and  $\mathbb{E}[\mathbf{x}\mathbf{x}^H] = \mathbf{I}_K$ . For that case,  $\sqrt{Q}$  is an integer and  $\mathcal{X} \triangleq \{x_I + jx_Q : x_I, x_Q \in \mathcal{S}\}$ , where  $\mathcal{S} \triangleq \left\{ \sqrt{\frac{3}{2(Q-1)}}(2q-1-\sqrt{Q}) \right\}_{q=1}^{\sqrt{Q}}$  is the constellation of  $\sqrt{Q}$ -PAM. Each wireless link is subject to Rayleigh small-scale fading, i.e., channel vectors  $\mathbf{h}_k \sim \mathcal{CN}(\mathbf{0}_M, v_k^2 \mathbf{I}_M)$ , where  $v_k^2$  is the corresponding distance-dependent wireless channel variance. The resulting signal-to-noise ratio (SNR) for UE  $k$  is  $\text{SNR}_k \triangleq \frac{p_k v_k^2}{\sigma^2}$ .

For a simplified exposition, the signal model in Eq. (1) is transformed to the real domain as follows

$$\mathbf{r} = \mathbf{G}\mathbf{s} + \mathbf{w}, \quad (2)$$

where  $\mathbf{r} \triangleq \begin{bmatrix} \Re\{\mathbf{y}\} \\ \Im\{\mathbf{y}\} \end{bmatrix}$ ,  $\mathbf{G} \triangleq \begin{bmatrix} \Re\{\mathbf{HP}\} & -\Im\{\mathbf{HP}\} \\ \Im\{\mathbf{HP}\} & \Re\{\mathbf{HP}\} \end{bmatrix}$ ,  $\mathbf{s} \triangleq \begin{bmatrix} \Re\{\mathbf{x}\} \\ \Im\{\mathbf{x}\} \end{bmatrix}$ , and  $\mathbf{w} \triangleq \begin{bmatrix} \Re\{\mathbf{n}\} \\ \Im\{\mathbf{n}\} \end{bmatrix}$ . Note that  $\mathbf{r}, \mathbf{w} \in \mathbb{R}^{2M}$ ,  $\mathbf{G} \in \mathbb{R}^{2M \times 2K}$ , while each element of  $\mathbf{s}$  belongs to a  $\sqrt{Q}$ -PAM constellation, i.e.,  $\mathbf{s} \in \mathcal{S}^{2K}$ .

BS applies one-bit quantization on the signal  $\mathbf{r}$  and forms vector  $\mathbf{b} = [b_1 b_2 \dots b_{2M}]^T = \text{sign}(\mathbf{r}) \in \{\pm 1\}^{2M}$ , where  $\text{sign}(\cdot)$  is the sign operator applied component-wise. The objective at the BS is to detect  $\mathbf{s}$ , i.e., the transmitted symbol sequence from the UEs in the cell, using only the one-bit-quantized noisy measurements  $\mathbf{b}$ . The noise vector in (2) satisfies  $\mathbf{w} \sim \mathcal{N}(\mathbf{0}_{2M}, \frac{\sigma^2}{2} \mathbf{I}_{2M})$ , and thus, with the compound uplink channel matrix  $\mathbf{G} = [\mathbf{g}_1 \mathbf{g}_2 \dots \mathbf{g}_{2M}]^T$  available, the received vector offers the following statistics  $\mathbf{r} \sim \mathcal{N}(\mathbf{G}\mathbf{s}, \frac{\sigma^2}{2} \mathbf{I}_{2M})$ . Each element of  $\mathbf{b}$ ,  $b_m$ , follows Bernoulli distribution with  $\mathbb{P}(b_m = 1) = \mathcal{Q}\left(-\frac{\sqrt{2}}{\sigma} \mathbf{g}_m^T \mathbf{s}\right)$ , where  $\mathcal{Q}(x) = \frac{1}{\sqrt{2\pi}} \int_x^\infty e^{-t^2/2} dt$  is the well known Q-function. Using similar reasoning with [6, Eq. (4)], it follows that the SER-optimal ML detector can be expressed as

$$\hat{\mathbf{s}}^{\text{ML}} = \arg \min_{\mathbf{s} \in \mathcal{S}^{2K}} \left\{ - \sum_{m=1}^{2M} \ln \mathcal{Q}(-\sqrt{\gamma} b_m \mathbf{g}_m^T \mathbf{s}) \right\}, \quad (3)$$

where  $\gamma = 2/\sigma^2$ . The complexity to calculate the sequence  $\hat{\mathbf{s}}^{\text{ML}}$  in Eq. (3) scales as  $O(\sqrt{Q}^{2K} M K) = O(Q^K M K)$ , which is exponential on the number of UEs.

### III. PROPOSED NEAR SER-OPTIMAL DETECTOR

In this section a two-phase detection algorithm is proposed in order to seek an approximate solution to the ML detector in (3), which requires exponential computational cost.

#### A. Phase I: Relaxation and Projection

In the first phase (phase I), a convex surrogate of optimization problem (3) is formulated. Specifically, since each element of  $\mathbf{s}$ ,  $s_n$ , belongs to a  $\sqrt{Q}$ -PAM constellation, we relax constraint  $\mathbf{s} \in \mathcal{S}^{2K}$  to  $|s_n| \leq \sqrt{\frac{3}{2(Q-1)}}(\sqrt{Q}-1)$ ,  $n = 1, 2, \dots, 2K$ . Hence, the proposed convex relaxation version of (3) is expressed as

$$\underset{\mathbf{s} \in \mathbb{R}^{2K}}{\text{minimize}} \quad - \sum_{m=1}^{2M} \ln \mathcal{Q}(-\sqrt{\gamma} b_m \mathbf{g}_m^T \mathbf{s}) \quad (4a)$$

$$\text{subject to } |s_n| \leq \sqrt{\frac{3(\sqrt{Q}-1)^2}{2(Q-1)}}, \quad n = 1, 2, \dots, 2K. \quad (4b)$$

Note that function  $f(\mathbf{s}) \triangleq -\sum_{m=1}^{2M} \ln \mathcal{Q}(-\sqrt{\gamma} b_m \mathbf{g}_m^T \mathbf{s})$  is a convex function of  $\mathbf{s} \in \mathbb{R}^{2K}$  as a composition of an affine function with a convex increasing function  $-\ln \mathcal{Q}(x)$  [7, p. 84]. The set of constraints in Eq. (4b) is denoted as  $\mathcal{B}$ , i.e.,  $\mathcal{B} \triangleq \left\{ \mathbf{s} \in \mathbb{R}^{2K} : |s_n| \leq \sqrt{\frac{3(\sqrt{Q}-1)^2}{2(Q-1)}}, n = 1, 2, \dots, 2K \right\}$ , forming a box on  $\mathbb{R}^{2K}$ , which is a convex set. Thus, the problem in (4) is a convex optimization problem [7], which can be solved either with gradient- or Newton-based iterative algorithms.

In this work, the optimal solution of problem (4) is calculated through an accelerated projected gradient method exploiting the smoothness of the objective function (i.e., continuously differentiable objective) [8]. First, the gradient of  $f(\cdot)$  is calculated as [9]

$$\nabla f(\mathbf{s}) = - \sum_{m=1}^{2M} \frac{\sqrt{\gamma} b_m e^{-\frac{\gamma(\mathbf{g}_m^T \mathbf{s})^2}{2}}}{\sqrt{2\pi} \mathcal{Q}(-\sqrt{\gamma} b_m \mathbf{g}_m^T \mathbf{s})} \mathbf{g}_m. \quad (5)$$

Then, we need to evaluate an upper bound for local smoothness parameter of function  $f(\mathbf{s})$  at any  $\mathbf{s} \in \mathbb{R}^{2K}$ , which through the use of Cauchy-Swartz inequality for matrix norms, can be obtained as [9]:  $\|\nabla^2 f(\mathbf{s})\|_2 \leq \|\mathbf{G}\|_2^2 \|\mathbf{d}(\mathbf{s})\|_\infty \triangleq L(\mathbf{s})$ ,  $\forall \mathbf{s} \in \mathbb{R}^{2K}$ , where the elements of vector function  $\mathbf{d}(\mathbf{s})$  are given by

$$d_m(\mathbf{s}) = \frac{\gamma e^{-\gamma(\mathbf{g}_m^T \mathbf{s})^2}}{2\pi [\mathcal{Q}(-\sqrt{\gamma} b_m \mathbf{g}_m^T \mathbf{s})]^2} + \frac{\gamma^{\frac{3}{2}} b_m (\mathbf{g}_m^T \mathbf{s}) e^{-\frac{\gamma(\mathbf{g}_m^T \mathbf{s})^2}{2}}}{\sqrt{2\pi} \mathcal{Q}(-\sqrt{\gamma} b_m \mathbf{g}_m^T \mathbf{s})}, \quad (6)$$

$m = 1, 2, \dots, 2M$ . Note that for any  $\mathbf{s} \in \mathbb{R}^{2K}$ , function  $L(\mathbf{s})$  is an upper bound for the local smoothness parameter of function  $f(\cdot)$ .

For the problem in (4), classic projected gradient method iterates as  $\mathbf{s}^{(t+1)} = \mathbf{P}_{\mathcal{B}}(\mathbf{s}^{(t)} - \eta \nabla f(\mathbf{s}^{(t)}))$  until convergence, where  $\mathbf{P}_{\mathcal{B}}(\cdot)$  is the projector operator onto the set  $\mathcal{B}$ , given by

$$[\mathbf{P}_{\mathcal{B}}(\mathbf{s})]_n = \text{sign}(s_n) \min \left\{ |s_n|, \sqrt{\frac{3(\sqrt{Q}-1)^2}{2(Q-1)}} \right\}, \quad (7)$$

$n = 1, 2, \dots, 2K$ , and  $\eta$  is a suitable constant gradient step size. On the other hand, the proposed accelerated projected gradient method: (a) exploits the knowledge of local smoothness upper bound  $L(\cdot)$  in the calculation of the gradient step size and (b) employs an extra extrapolation step after projection. More specifically, the proposed accelerated projected gradient procedure is shown in Algorithm 1.

At line (4), the upper bound of local smoothness parameter of  $f(\cdot)$ ,  $L(\cdot)$ , is calculated, exploiting the fact that  $\|\mathbf{G}\|_2^2$  can be precomputed. At line (5), a projected gradient step is applied, where the gradient step size harnesses the knowledge of  $L(\cdot)$  at the current point. Lines (6) and (7) calculate the optimal interpolation parameter  $\beta^{(t+1)}$  [8] and apply the interpolation step between the current and the previous points, respectively. Since function  $f(\cdot)$  is smooth, executing lines (4) to (7) iteratively until convergence, an  $\epsilon$ -optimal solution can be found (a neighborhood of the optimal solution with diameter  $\epsilon \ll 1$ ) using at most  $O(1/\sqrt{\epsilon})$  iterations [8]. An adaptive restart mechanism (at lines 8–10) is also utilized [10] in order to further speed up the convergence rate, requiring also at most  $O(1/\sqrt{\epsilon})$  iterations to reach an  $\epsilon$ -optimal solution

---

**Algorithm 1** Algorithm to solve problem (4)
 

---

**Input:**  $\mathbf{G}, \mathbf{b}, \gamma$ 

```

1: Pre-compute  $\|\mathbf{G}\|_2^2$ 
2:  $t = 0$  : Initialize  $\beta^{(0)} = 1$ ,  $\mathbf{u}^{(0)} = \mathbf{s}^{(0)} \in \mathbb{R}^{2K}$ 
3: while Stopping criterion is not reached do
4:    $\mathbf{L}(\mathbf{u}^{(t)}) = \|\mathbf{G}\|_2^2 \|\mathbf{d}(\mathbf{u}^{(t)})\|_\infty$ 
5:    $\mathbf{s}^{(t+1)} = \mathcal{P}_{\mathcal{B}}\left(\mathbf{u}^{(t)} - \frac{1}{\mathbf{L}(\mathbf{u}^{(t)})} \nabla f(\mathbf{u}^{(t)})\right)$ 
6:    $\beta^{(t+1)} = \frac{1 + \sqrt{1 + 4(\beta^{(t)})^2}}{2}$ 
7:    $\mathbf{u}^{(t+1)} = \mathbf{s}^{(t+1)} + \frac{\beta^{(t)} - 1}{\beta^{(t+1)}} (\mathbf{s}^{(t+1)} - \mathbf{s}^{(t)})$ 
8:   if  $\nabla f(\mathbf{u}^{(t)})^\top (\mathbf{s}^{(t+1)} - \mathbf{s}^{(t)}) > 0$  then
9:      $\beta^{(t+1)} = 1$ ,  $\mathbf{u}^{(t+1)} = \mathbf{s}^{(t+1)}$ 
10:  end if
11:   $t := t + 1$ 
12: end while

```

**Output:**  $\hat{\mathbf{s}}^{(1)} = \mathbf{s}^{(t)}$ 


---

[11]. The algorithm terminates either if quantity  $\frac{\|\mathbf{s}^{(t+1)} - \mathbf{s}^{(t)}\|_2}{\|\mathbf{s}^{(t)}\|_2}$  is below a prescribed precision or if a maximum number of iterations is reached. In contrast, the projected gradient scheme with constant step size, converges to an optimal solution after  $O(1/\epsilon)$  iterations, which is much larger than the proposed  $O(1/\sqrt{\epsilon})$ , especially for small  $\epsilon$ .

The calculation of  $\|\mathbf{G}\|_2^2$  requires  $O(K^2 M)$  arithmetic operations. The per iteration complexity of the proposed algorithm is  $O(KM)$  due to the evaluation of  $\nabla f(\mathbf{u}^{(t)})$  and  $\mathbf{d}(\mathbf{u}^{(t)})$  at lines 4 and 5, respectively. In the worst case, the algorithm iterates  $I_{\max} \approx 1/\sqrt{\epsilon}$  times to find an  $\epsilon$ -optimal solution, requiring computational cost  $O(\frac{1}{\sqrt{\epsilon}} KM)$ . Thus, the overall computational cost for Algorithm 1 is  $O(KM(1/\sqrt{\epsilon} + K))$ .

As the elements of the  $\epsilon$ -optimal solution vector  $\hat{\mathbf{s}}^{(1)}$  are soft estimates that do not necessarily belong to the  $\sqrt{Q}$ -PAM constellation set, after the execution of Algorithm 1 a nearest neighbor rule is employed, by projecting each element of  $\hat{\mathbf{s}}^{(1)}$ ,  $\hat{s}_n^{(1)}$ , to the constellation set  $\mathcal{S}$ , i.e.,

$$\hat{s}_n^{(1)} = \arg \min_{s \in \mathcal{S}} |\hat{s}_n^{(1)} - s|, \quad n = 1, 2, \dots, 2K. \quad (8)$$

Note that  $\hat{\mathbf{s}}^{(1)} \in \mathcal{S}^{2K}$  and also, by the properties of ML detector,  $f(\hat{\mathbf{s}}^{(1)}) \geq f(\hat{\mathbf{s}}^{\text{ML}})$  holds.

### B. Phase II: Refinement and Multiuser Detection

In the second phase (phase II) of the proposed algorithm we apply a refinement step to further improve detection performance. First, the vector of absolute residuals is formed as

$$z_n \triangleq |\hat{s}_n^{(1)} - \hat{s}_n^{(1)}|, \quad n = 1, 2, \dots, 2K. \quad (9)$$

The elements of vector  $\mathbf{z}$  express the absolute mismatch of the soft-decision estimates and the projected estimates of phase I. Intuitively, the smaller the value of a  $z_n$  is, the more reliable is the estimate for  $\hat{s}_n^{(1)}$ , in the sense that  $\hat{s}_n^{(1)} = \hat{s}_n^{\text{ML}}$  with high probability.

After forming vector  $\mathbf{z}$ , we choose the  $R$  largest elements of  $\mathbf{z}$ . Parameter  $R$  is a refinement parameter, determining how many elements of estimated vector  $\hat{\mathbf{s}}^{(1)}$  and ML vector  $\hat{\mathbf{s}}^{\text{ML}}$  may be different. Refining the decision on the elements of decision

vector  $\hat{\mathbf{s}}^{(1)}$ , corresponding to the indexes of the  $R$  largest (less-reliable) elements of vector  $\mathbf{z}$ , can in principle boost the SER performance of the detector. Let us denote  $\mathcal{J}_r \subset \{1, 2, \dots, 2K\}$  the set of indexes associated with the  $R$  largest elements of residual vector  $\mathbf{z}$ . For each unreliable residual element, i.e.,  $n \in \mathcal{J}_r$ , the second closest symbol from the  $\sqrt{Q}$ -PAM constellation is obtained through

$$\hat{s}_n^{(\text{II})} = \arg \min_{s \in \mathcal{S} \setminus \hat{s}_n^{(1)}} |\hat{s}_n^{(1)} - s|, \quad n \in \mathcal{J}_r. \quad (10)$$

The two closest points of  $\mathcal{S}$  to the soft-decision estimate  $\hat{s}_n^{(1)}$ , i.e.,  $\{\hat{s}_n^{(1)}, \hat{s}_n^{(\text{II})}\}$ , are the refined candidate decision estimates of symbol  $s_n$ , for  $n \in \mathcal{J}_r$ . On the other hand, for  $n \in \{1, 2, \dots, 2K\} \setminus \mathcal{J}_r$ , only the closest point of  $\mathcal{S}$  to the soft-decision estimate  $\hat{s}_n^{(1)}$  (i.e., only  $\{\hat{s}_n^{(1)}\}$ , obtained from (8)), constitutes the single candidate decision estimate for symbol  $s_n$ . Combining the above, the refined symbols' codebook can be mathematically expressed as

$$\mathcal{W}_r = \bigotimes_{n \notin \mathcal{J}_r} \{\hat{s}_n^{(1)}\} \times \bigotimes_{n \in \mathcal{J}_r} \{\hat{s}_n^{(1)}, \hat{s}_n^{(\text{II})}\}, \quad (11)$$

forming a set of  $2^R$   $2K$ -dimensional  $\sqrt{Q}$ -PAM symbol sequences. After forming the refined symbols' codebook, the final detector is given by

$$\hat{\mathbf{s}} = \arg \min_{\mathbf{s} \in \mathcal{W}_r} \left\{ - \sum_{m=1}^{2M} \ln Q(-\sqrt{\gamma} b_m \mathbf{g}_m^\top \mathbf{s}) \right\}. \quad (12)$$

The total computational cost to evaluate the detection rule in (12) is  $O(MK2^R)$ . After obtaining  $\hat{\mathbf{s}}$ , BS reconstructs the transmitted complex  $Q$ -QAM symbols from all  $K$  UEs as:  $\hat{x}_k = \hat{s}_k + j\hat{s}_{K+k}$ ,  $k = 1, 2, \dots, K$ .

### C. Remarks

The overall computational cost for the end-to-end multiuser detection procedure, described in phase I and phase II above, scales with  $O(MK(2^R + 1/\sqrt{\epsilon} + K))$ , which is not exponential on the number of UEs, depending exponentially on the refinement parameter. The latter controls the accuracy versus complexity trade-off. In the studied simulation setups, we found that the proposed detector can attain very close SER performance to the ML detector even for small values of parameter  $R$ .

## IV. NUMERICAL RESULTS

For the studied simulation setups, the SER performance of the following schemes is studied: (i) proposed two-phase detector, (ii) the detector in [3] (two-stage nML), (iii) the detector in [4] (1-bit ZF), implementable only for 4-QAM, (iv) the Bussgang linear minimum mean-squared error (BLMMSE) detector, that estimates a soft-decision version of transmitted vector  $\mathbf{x}$  using the framework presented in [12] and the elements of the outcome are projected to the  $Q$ -QAM constellation set, and (v) the ML detector. The two-stage detector in [3] requires  $O(MK(1/\epsilon))$  arithmetic operations for first stage plus  $O(MK4^K)$  arithmetic operations for the second stage, using common neighborhood parameter  $c$  for all sets in [3, Eq. (38)];

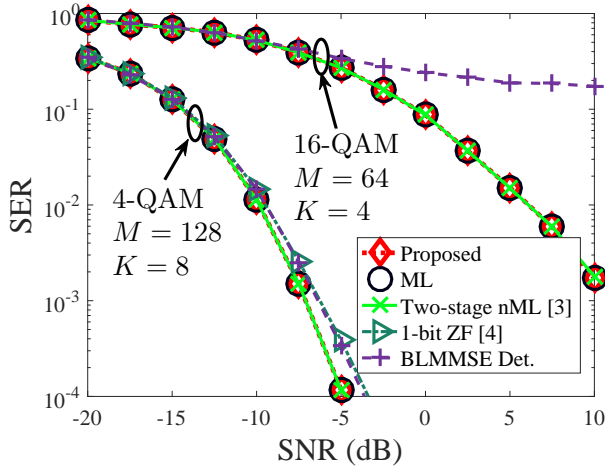


Fig. 1. SER as a function of SNR.

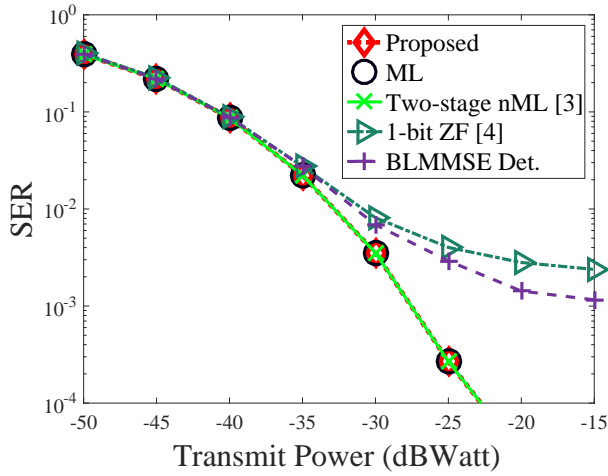


Fig. 2. SER as a function of transmit power.

in contrast to the proposed scheme, the required complexity in [3] is exponential on the number of UEs. The computational cost of BLMMSE detector is  $O(M^2(M+K))$ , while the simple linear detector in [4] requires  $O(MK^2)$  arithmetic operations. The proposed detection technique employs  $R = 4$  and  $R = 6$  for the 4-QAM and 16-QAM systems, respectively.

In the first simulation study of Fig. 1 the SER is plotted as a function of SNR, using  $p_k = 1$  and  $v_k^2 = 1$ , for  $k = 1, 2, \dots, K$ , examining also the impact of parameters  $K$ ,  $M$ , and QAM modulation order,  $Q$ . For the 4-QAM and 16-QAM systems, the SER of the proposed and the two-stage nML detectors coincide with the SER of the ML detector. The ZF 1-bit detector works only for 4-QAM, while for 16-QAM the resulting SER is larger than 0.5; the algorithm is computationally cheap but its SER performance compared to the other detectors is worse, especially for high SNR. The BLMMSE detector slightly outperforms ZF 1-bit detector and offers slightly worse SER than near ML detectors for the 4-QAM system, while for 16-QAM system its SER cannot drop below 10%. The proposed detector achieves near optimal performance requiring significantly less computational cost compared to the two-stage nML detector.

In the next simulation setup of Fig. 2 we consider a BS with  $M = 150$  antennas, placed at  $[0 \ 0 \ 100]^T$ , and  $K = 8$  UEs transmitting 4-QAM symbols, that are randomly placed around the BS. The average SER performance of the UEs is examined as a function of the UE transmit power, using  $p_k = p$ , for  $k = 1, 2, \dots, K$ . The following path-loss model is considered:  $v_k^2 = (\lambda/4\pi)^2 (d_k/d_0)^\nu$ , with  $d_0 = 100$  meters,  $\nu = 3.2$ ,  $\lambda = 0.15$ , where  $d_k$  denotes the distance from the  $k$ th UE to the BS. The noise power was set  $\sigma^2 = -130$  dBWatt.

In this asymmetric multiuser setting, the SER of 1-bit ZF detector saturates after  $p = -20$  dBWatt transmit power. BLMMSE detector slightly outperforms 1-bit ZF and its SER also saturates after  $p = -20$  dBWatt. The saturation effect stems from the fact that the channel matrix is ill-conditioned and at the high-power regime, BLMMSE and 1-bit ZF detectors may offer some erroneous detection decisions due to the required channel inversion. Both BLMMSE and 1-bit ZF detectors offer similar SER with nML detectors, but beyond  $p = -30$  dBWatt their performance becomes worse. On the other hand, the proposed and the two-stage nML detectors achieve similar SER with the optimal ML detector.

## V. CONCLUSION

In this work a two-phase detection algorithm is proposed for uplink multiuser massive MIMO systems employing single-bit ADCs. The algorithm achieves the SER performance of the ML detector and manages to significantly reduce the computational cost of the nML detectors in prior art.

## REFERENCES

- [1] S. Wang, Y. Li, and J. Wang, "Multiuser detection for uplink large-scale MIMO under one-bit quantization," in *Proc. IEEE Int. Conf. on Commun. (ICC)*, Sydney, NSW, Australia, 2014, pp. 4460–4465.
- [2] S. Jacobsson, G. Durisi, M. Coldrey, U. Gustavsson, and C. Studer, "One-bit massive MIMO: Channel estimation and high-order modulations," in *Proc. IEEE Int. Conf. on Commun. (ICC)*, London, UK, 2015, pp. 1304–1309.
- [3] J. Choi, J. Mo, and R. W. Heath, "Near maximum-likelihood detector and channel estimator for uplink multiuser massive MIMO systems with one-bit ADCs," *IEEE Trans. Commun.*, vol. 64, no. 5, pp. 2005–2018, May 2016.
- [4] C. Risi, D. Persson, and E. G. Larsson, "Massive MIMO with 1-bit ADC," 2014. [Online]. Available: [arxiv.org/pdf/1404.7736](http://arxiv.org/pdf/1404.7736)
- [5] E. Dahlman, S. Parkvall, and J. Skold, *4G, LTE-Advanced Pro and The Road to 5G*. Elsevier Science, 2016.
- [6] E. Tsakonas, J. Jaldén, N. D. Sidiropoulos, and B. Ottersten, "Sparse conjoint analysis through maximum likelihood estimation," *IEEE Trans. Signal Process.*, vol. 61, no. 22, pp. 5704–5715, Nov. 2013.
- [7] S. Boyd and L. Vandenberghe, *Convex Optimization*. New York, NY, USA: Cambridge University Press, 2004.
- [8] S. Bubeck, "Convex optimization: Algorithms and complexity," *Foundations and Trends® in Machine Learning*, vol. 8, no. 3-4, pp. 231–357, 2015.
- [9] P. N. Alevizos, X. Fu, N. Sidiropoulos, Y. Yang, and A. Bletsas, "Limited feedback channel estimation in massive MIMO with non-uniform directional dictionaries," 2018. [Online]. Available: [arxiv.org/pdf/1712.10085](http://arxiv.org/pdf/1712.10085)
- [10] B. O'Donoghue and E. Candès, "Adaptive restart for accelerated gradient schemes," *Foundations of Computational Mathematics*, vol. 15, no. 3, pp. 715–732, 2015.
- [11] P. Giselsson and S. Boyd, "Monotonicity and restart in fast gradient methods," in *Proc. IEEE Conference on Decision and Control*, Los Angeles, CA, Dec. 2014, pp. 5058–5063.
- [12] Y. Li, C. Tao, G. Seco-Granados, A. Mezghani, A. L. Swindlehurst, and L. Liu, "Channel estimation and performance analysis of one-bit massive MIMO systems," *IEEE Trans. Signal Process.*, vol. 65, no. 15, pp. 4075–4089, May 2017.